# Degradation of Perfluoroalkyl Ether Carboxylic Acids (PFECAs) with Hydrated Electrons: Structure-Reactivity Relationships and Environmental Implications

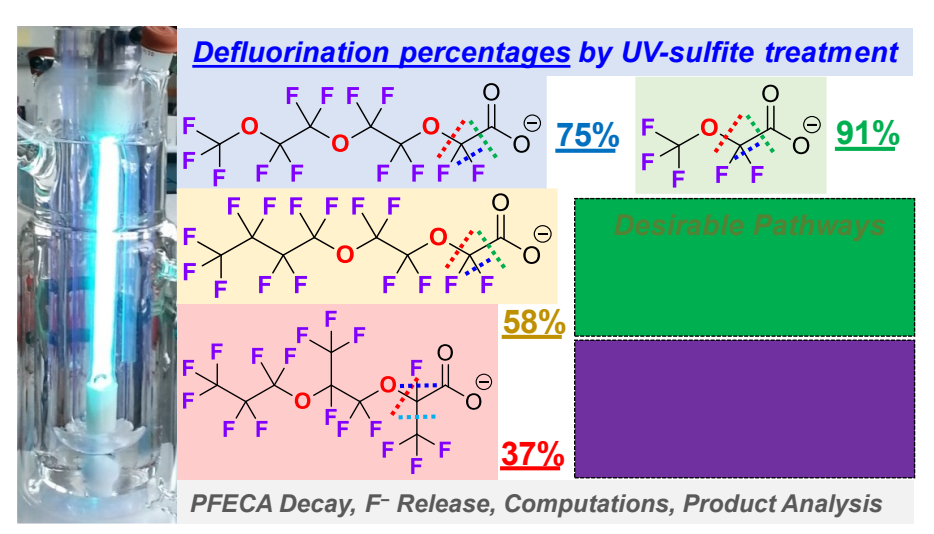
Michael J. Bentel,<sup>†</sup> Yaochun Yu,<sup>§</sup> Lihua Xu,<sup>†</sup> Hyuna Kwon,<sup>†</sup> Zhong Li,<sup>||</sup> Bryan M. Wong,<sup>†,‡</sup> Yujie Men, <sup>†,§,†</sup> and Jinyong Liu\*,<sup>†</sup>

<sup>†</sup>Department of Chemical & Environmental Engineering and <sup>‡</sup>Materials Science & Engineering Program, University of California, Riverside, California, 92521, United States

<sup>§</sup>Department of Civil & Environmental Engineering, Metabolomics Lab of Roy J. Carver Biotechnology Center, and Linstitute for Genomic Biology, University of Illinois at Urbana−Champaign, Urbana, Illinois, 61801, United States

9 ABSTRACT

This study explores structure-reactivity relationships for the degradation of emerging perfluoroalkyl ether carboxylic acid (PFECA) pollutants with UV-generated hydrated electrons ( $e_{aq}^-$ ). The rate and extent of PFECA degradation depend on both the branching extent and the chain length of oxygen-segregated fluoroalkyl moieties. Kinetic measurements, theoretical calculations, and transformation product analyses provide a comprehensive understanding of PFECA degradation mechanisms and pathways. In comparison to the traditional full-carbon-chain perfluorocarboxylic acids (PFCAs), the distinct degradation behavior of PFECAs is attributed to their ether structures. The ether oxygen atoms elevate the bond dissociation energy (BDE) of the C-F bonds on the adjacent  $-CF_2$ - moieties. This impact reduces the formation of H/F-exchanged polyfluorinated products that are recalcitrant to reductive defluorination. Instead, the cleavage of ether C-O bonds generates unstable perfluoroalcohols and thus promotes deep defluorination of short fluoroalkyl moieties. In comparison to linear PFECAs, branched PFECAs has a higher tendency of H/F exchange on the tertiary carbon and thus lower percentages of defluorination. These findings provide mechanistic insights for an improved design and efficient degradation of fluorochemicals.



## INTRODUCTION

26

27

28

29

30

31

32

33

34

35

36

37

38

39

40

41

42

43

44

45

46

47

48

Since the 1940s, per- and polyfluoroalkyl substances (PFASs) have been extensively used in a wide range of applications due to their unique properties (e.g., hydrophobicity, lipophobicity, and thermal stability) as well as their relative ease in chemical design and synthesis. 1-5 The highly stable C-F bonds make PFAS molecules recalcitrant to natural and engineered degradation,<sup>6</sup> leading to global PFAS pollution<sup>7</sup> and worldwide efforts on PFAS regulation.<sup>8-11</sup> Fluorochemical industries have been phasing out the production and use of some legacy PFASs (e.g., PFOA)<sup>2, 12</sup> due to their heavy pollution to the environment and high toxicities to humans. 13, 14 Perfluoroalkyl ether carboxylic acids (PFECAs) that contain ether C-O bonds in molecules have been developed as "less bioaccumulative alternatives" to the full-carbon-chain predecessor PFASs. 15 However, as toxicological studies have revealed even higher bioaccumulation potential and toxicity of some PFECAs than PFOA, 16-19 PFECAs have been recognized as a new class of contaminants of emerging concern (Figure 1).<sup>20-23</sup> At some sites in North America and in Europe, PFECAs have been detected in much higher concentrations than legacy PFASs. 24, 25 Furthermore, due to the facile synthesis of PFECAs from a flexible choice of fluoroalkene oxide building blocks (e.g., SI Figure S1)<sup>26</sup> and the formation of byproducts, <sup>27</sup> the diversity of PFECA contaminants identified in the environment has been rapidly increasing. <sup>27-29</sup>

While physical separation methods (e.g., carbon adsorption, ion exchange, and membrane filtration) enable rapid PFAS removal from contaminated water,<sup>30</sup> concentrated PFASs in the carbon/resin regeneration wastes and membrane rejects still need degradation treatment. Various novel methods, such as electrochemical,<sup>31</sup> sonochemical,<sup>32</sup> radiolytic,<sup>33</sup> plasmatic,<sup>34</sup> and other oxidative and reductive approaches,<sup>30, 35</sup> have been primarily developed for the degradation of PFOA and PFOS. A few studies have investigated the destruction of selected PFECAs, including

sonochemical oxidation with persulfate,<sup>36</sup> photocatalytic oxidation with phosphotungstic acid under pressurized  $O_2$ ,<sup>37</sup> and reduction with UV-generated hydrated electrons ( $e_{aq}^-$ ).<sup>38,39</sup> These early studies have revealed a variety of mechanistic insights on PFECA degradation. In particular, reductive degradation of branched PFECAs (e.g., GenX in **Figure 1**) using  $e_{aq}^-$  is much more effective than oxidative degradation using sulfate radicals.<sup>38, 39</sup> However, a systematic understanding of reaction pathways and structure-reactivity relationships has not yet been established.

49

50

51

52

53

54

55

56

57

58

59

60

61

62

63

64

65

66

67

68

69

70

Recently, our research team has systematically studied the reductive defluorination of fullcarbon-chain PFASs by  $e_{\mathrm{aq}}^-$  produced from aqueous sulfite under UV irradiation. The degradation mechanisms for perfluorocarboxylic acids (PFCAs) and fluorotelomer carboxylic acids (FTCAs) are significantly different. FTCAs (R<sub>F</sub>-CH<sub>2</sub>CH<sub>2</sub>-COO<sup>-</sup>, R<sub>F</sub> representing the fluorocarbon moiety) are much more recalcitrant than PFCAs (R<sub>F</sub>-COO<sup>-</sup>), especially when the chain length of  $R_F$  is short. The incomplete defluorination of PFCAs can also be attributed to the formation of polyfluorinated R<sub>F</sub>-CH<sub>2</sub>-COO<sup>-</sup> products.<sup>40</sup> These findings indicate the importance of a direct linkage between R<sub>F</sub> and -COO<sup>-</sup> to allow an effective degradation of full-carbon-chain PFASs using  $e_{aq}$ . In comparison, the flexible incorporation of ether linkages in PFECAs generates various oxygen-segregated fluoroalkyl moieties, which can be either branched or linear in variable lengths. This novel structural diversity raises fundamental questions regarding mechanistic understanding and pollution control: (1) Mechanistically, what roles do the ether C-O bond and other structural features play in PFECA degradation using  $e_{aq}^{-}$ ? (2) Practically, in comparison to full-carbon-chain PFCAs, can PFECAs be treated in higher effectivity by the promising reductive technologies?

To answer these questions, we investigated the reductive defluorination of ten PFECAs with (i) varying numbers of ether C–O bonds, (ii) varying chain lengths of oxygen-segregated fluoroalkyl moieties, and (iii) branched versus linear fluoroalkyl structures. To achieve a comprehensive understanding, we conducted kinetic measurements on parent compound decay and fluoride ion (F<sup>-</sup>) release, theoretical calculations on C–F / C–O bond dissociation energies and spontaneous bond cleavage upon reaction with  $e_{\rm aq}$ , and transformation product analyses with high-resolution mass spectrometry. These results collectively reveal and confirm novel mechanistic insights into PFECA degradation. The findings will advance the treatment technologies for existing PFECA pollutants and facilitate the molecular design of fluorochemicals with enhanced degradability.

#### MATERIAL AND METHODS

This study used ten PFECAs with fine-tuned structural variability in four categories (*A1* through *D2* in Table 1) and two special compounds (trifluoropyruvate CF<sub>3</sub>–CO–COO<sup>-</sup> and polyfluorinated CF<sub>3</sub>–O–CH<sub>2</sub>–COO<sup>-</sup>) for mechanistic investigation. Detailed information on these chemicals is included in the Supporting information (SI). Preparation of PFECA stock solutions, photochemical reaction settings, sample analysis, and theoretical calculations have been fully described in our previous work (Open Access).<sup>40</sup> We used consistent reaction conditions to compare the degradation behavior between PFECAs and traditional full-carbon-chain PFCAs. Briefly, photochemical degradation of individual PFECAs was carried out in 600-mL closed-system batch reactors equipped with a low-pressure mercury lamp (254 nm, 18 W, enclosed in a quartz immersion well). Both the reactor and immersion well were connected to circulating cooling water at 20°C. The reaction mixture contained 25 μM of PFECA, 10 mM of Na<sub>2</sub>SO<sub>3</sub>, and 5 mM of NaHCO<sub>3</sub>, and the pH was adjusted to 9.5 with NaOH. Released F<sup>-</sup> was measured with an ion-

selective electrode, which has been validated for the quantification accuracy by ion chromatography. All reactions were conducted in triplicates of operations from the preparation of stock solution to the quantification of defluorination percentage (deF%), which is defined as

97 
$$deF\% = \frac{c_{F^-}}{c_{0}*N_{C-F}} \times 100\%$$
 (1)

where  $C_F^-$  is the molar concentration of  $F^-$  ion released in solution,  $C_0$  is the initial molar concentration of the parent PFECAs, and  $N_{C-F}$  is the number of C-F bonds in the parent PFECA molecule. Reaction samples were analyzed with a liquid chromatography-triple quadrupole mass spectrometer (LC-MS/MS) for the quantification of parent compounds and transformation products that have pure chemicals available as analytical standards, as well as a liquid chromatography-high resolution mass spectrometer (LC-HRMS) for the screening of transformation products without analytical standards. The quality assurance and quality control of MS analyses have been addressed previously,  $^{40}$  with new details provided in the SI for the PFECA degradation samples. Small ionic species including trifluoroacetate, trifluoropyruvate, oxalate,  $CF_3-O-CF_2-COO^-$ , and  $CF_3-O-CH_2-COO^-$  were analyzed by ion chromatography (IC) equipped with a conductivity detector (specific separation conditions are described in the SI).

## **RESULTS AND DISCUSSION**

**PFCAs.** Figure 2 shows the decay and defluorination of four PFASs representing full-carbon-chain PFCAs, linear PFECAs, and branched PFECAs. The parent compound decay is the fastest for the two traditional PFCAs and the slowest for the branched PFECA (**Figure 2a**). The order of parent compound decay rates for these structures does not match the order of their defluorination percentages. **Figure 2b** shows distinct defluorination profiles between PFECAs and traditional

PFCAs, as well as between the linear and branched PFECAs. All four PFASs showed an initial period of rapid F<sup>-</sup> release, followed by slower F<sup>-</sup> release before reaching a plateau. However, the initial rates of defluorination from the two PFECAs are slower than those from the two PFCAs. In particular, the linear PFECA showed a slower initial rate but a significantly deeper defluorination than PFHpA (i.e., 75% vs. 55% of the 13 F atoms in both molecules). In contrast, the branched PFECA showed both a slower rate and a less extent of defluorination than PFNA (i.e., 40% vs. 58% of the 17 F atoms in both molecules). These results suggest new structure-reactivity relationships governing PFECA degradation. To systematically understand the mechanisms, we extended the compound scope to ten individual PFECAs, which exhibited structure-specific profiles of parent compound decay and defluorination (**Table 1** and **Figure 3**).

Different Degradability of the Four PFECA Structure Categories. Category A includes structures AI-A3 with branched  $\neg$ CF<sub>3</sub> groups. They are the acid forms of hexafluoropropylene oxide dimer, trimer, and tetramer (HFPO-DA, HFPO-TrA, and HFPO-TeA), respectively. The initial rates of parent compound decay were similar (Figure 3a), but longer structures showed lower deF% (Figure 3b). The defluorination percentages of these branched PFECAs (31–45%) were significantly lower than that of traditional PFCAs (~55%) under the same reaction condition. Category B includes mono-ether structures BI-B3 with the CF<sub>3</sub>O- head group and linear  $\neg$ (CF<sub>2</sub>)<sub>n</sub>- moieties (n = 1, 2, and 3, respectively) before the terminal  $\neg$ COO- group. The decay of B2 and B3 finished within 12 h (Figure 3c), and the time profiles for their parent compound decay are similar to full-carbon-chain PFCAs (Figure 2a). The final defluorination percentages are also similar (61% and 52% for B2 and B3, respectively vs. 55% for PFCAs). In stark contrast, while the decay of B1 (n=1) was much slower than B2 and B3, the deF% was substantially higher (91%). From the kinetic data, it seems that these CF<sub>3</sub>-O-(CF<sub>2</sub>)<sub>n</sub>-COO-

structures behave similarly to F(CF<sub>2</sub>)<sub>n</sub>–COO<sup>-</sup> under reductive treatment. In our previous study,<sup>40</sup> the decay of CF<sub>3</sub>–COO<sup>-</sup> took 24 h to complete while the deF% was almost 100%, whereas the decay of all longer PFCAs took 8–12 hours to complete, but the maximal deF% was around 55% (**Table 1, entry E1** vs. **E2**).

We further tested two linear multi-ether PFECA categories, *C* and *D*. Both categories contain tetrafluoroethylene oxide (TFEO) building blocks, but the head groups are CF<sub>3</sub>O- and C<sub>4</sub>F<sub>9</sub>O-, respectively. With the -O-CF<sub>2</sub>-COOH as the ending group, the parent compound decay became slow again (**Figures 3e** and **3g**). Like the decay profile for the long molecule *A3* (**Figure 3a**), the decay of long molecule *D2* was also incomplete within 48 h. The other three structures *C1*, *C2*, and *D1* showed similar profiles of parent compound decay. The notable difference between these two PFECA categories is that, *C1* and *C2* with the short CF<sub>3</sub>O- head group yielded significantly higher deF% (82% and 75%, respectively) than *D1* and *D2* with the long C<sub>4</sub>F<sub>9</sub>O-head group (58% and 65%, respectively) (**Figures 3f** versus **3h**).

Structural Effects on PFECA Degradation. The kinetic data shown above have indicated the following characteristics of PFECA degradation in comparison to traditional PFCAs: (i) branched PFECAs showed slower decay and lower defluorination; (2) linear PFECAs showed slower decay if the end group is  $-O-CF_2-COO^-$ , or very similar rate of decay if more than one  $-CF_2-$  linkers are present in  $-O-(CF_2)_n-COO^-$ ; (3) linear PFECAs showed at least similar deF%, while those containing shorter oxygen-segregated fluoroalkyl moieties showed even higher deF%. To interpret these interesting results at the molecular level, we conducted theoretical calculations and transformation product analyses.

Theoretical Calculations of C-F and C-O Bond Dissociation Energies (BDEs). The BDEs of C-F and ether C-O bonds in all PFECA structures were calculated with density functional theory (DFT). Representative results are shown in Figure 4, and the full data sets are collected in SI Figures S2-S5. We identified new trends for C-F BDEs in PFECAs comparing to full-carbon-chain PFCAs. First, the ether oxygen elevates the BDE of C-F on the adjacent fluorocarbons. While the terminal –CF<sub>3</sub> in long fluoroalkyl chains has the typical C–F BDE <119 kcal mol<sup>-1</sup> (**Figures 4d**, **4f**, **4h** and **4i**), the inclusion of ether oxygen atoms increased the C-F BDE to 120–123 kcal mol<sup>-1</sup> (**Figures 4a–4c** and **g**). In fluorinated molecules, the ether oxygen acts as an electron-donating group like the -CH<sub>2</sub>- group in FTCAs (**Figure 4e**). With multiple oxygen atoms in the chain, the relatively weak C-F bonds in long-chain PFCAs were not found in linear PFECAs (Figure 4f versus 4g and 4h). In particular, the typical weak C-F bond at the αposition of PFCAs (i.e., BDE <108 kcal mol<sup>-1</sup>, **Figures 4d** and **4f**) does not exist in linear PFECAs with an ether oxygen at the  $\beta$ -position (i.e.,  $R_F$ -O-CF<sub>2</sub>-COO<sup>-</sup>, BDE >111 kcal mol<sup>-1</sup>, Figures 4a, **4g**, and **4h**). However, when the fluoroalkyl chain adjacent to  $-COO^-$  is longer (i.e., n = 2 or 3 in  $R_F$ -O-(CF<sub>2</sub>)<sub>n</sub>-COO<sup>-</sup>), the weak C-F bond at the  $\alpha$ -position appears again (Figures 4b and 4c). These novel trends on C-F BDEs in linear PFECAs corroborate the different rates of parent compound decay. The two structures with weak  $\alpha$ -position C-F bonds (B2 and B3 in Figure 3c) showed a similar rate of decay as the full-carbon-chain PFCAs (Figure 2a), while other  $R_F$ -O-CF<sub>2</sub>-COO structures showed slower parent compound decay (*B1*, *C1*, and *C2* in Figures 3c and 3e).

160

161

162

163

164

165

166

167

168

169

170

171

172

173

174

175

176

177

178

179

180

181

182

As for the branched PFECAs, the inclusion of ether oxygen atoms showed a similar effect on elevating the C-F BDEs. In comparison to a full-carbon-chain branched PFCA that contains very weak tertiary C-F bonds,<sup>41</sup> the oxygen atoms in HFPO-TrA significantly strengthen all

secondary and tertiary C-F bonds (**Figure 4i** versus **4j**). Although the HFPO oligomer acids contain distinctly weak tertiary C-F bonds (i.e., BDE <104 kcal mol<sup>-1</sup>), the rates of parent compound decay were slower than most of the linear PFECAs (**Figure 3**). Thus, other mechanisms and considerations beyond the cleavage of weak C-F bonds are likely responsible for the degradation of branched PFECAs.

183

184

185

186

187

188

189

190

191

192

193

194

195

196

197

198

199

200

201

202

203

204

205

As the cleavage of ether C-O bonds has been proposed for the degradation of HFPO-DA, <sup>38</sup>, <sup>39</sup> we further examined the BDEs of C-O bonds in all PFECAs. A very interesting phenomenon is the "asymmetric" strength of the two C-O bonds on the first ether linkage counted from the terminal -COO<sup>-</sup> (Figures 4k-4n). On this ether oxygen atom, the C-O bond away from -COO<sup>-</sup> has a considerably lower BDE (63–73 kcal mol<sup>-1</sup>) than the other one closer to –COO<sup>-</sup> (81–94 kcal mol<sup>-1</sup>). This phenomenon was observed in all PFECAs regardless of the total number of ether linkages, branched versus linear molecular backbone, or distance between -COO<sup>-</sup> and the first ether linkage (Figure 4k versus 4l). The BDE difference between those two C-O bonds in the three branched PFECAs ranges from 14.7 to 18.3 kcal mol<sup>-1</sup>, and the difference in linear PFECAs is even greater, from 19.8 to 23.3 kcal mol<sup>-1</sup> (see SI Figures S2–S5 for full data sets). However, if the PFECA molecule contains multiple ether oxygens, the pairs of C-O bonds in the remaining ether linkages have similar BDEs (i.e., only with small differences ranging from 0.1 to 3.4 kcal mol<sup>-1</sup>, **Figures 4m** and **4n**). In addition, due to the electron-withdrawing effect by -CF<sub>3</sub> branches, BDEs of these "normal" C-O bonds in branched multi-ether structures (82-84 kcal mol<sup>-1</sup>) are lower than those in linear multi-ether structures (89–97 kcal mol<sup>-1</sup>).

Spontaneous Bond Cleavage in Electron-Added PFECA Radical Anion Structures. The distinctly weak C-O in all PFECAs and relatively weak tertiary C-F bonds in branched PFECAs imply the potential cleavage of these bonds during the reaction. To verify this hypothesis, we

further conducted geometry optimization of the radical anion  $[R_F-COO]^{\bullet^2-}$  upon adding an extra electron (simulating the  $e_{aq}^-$ ) to the original PFECA anion  $(R_F-COO^-)^{.40}$  As expected, spontaneous stretching of  $\alpha$ -position C-F bonds (Figures 5a and 5b) and ether C-O bonds (Figures 5c and 5d) were observed. The distance between the two atoms went considerably longer than the normal length of C-O and C-F bonds (i.e., bond cleavage). The results for all PFECA structures are collected in SI Figures S6 and S7.

Interestingly, although the calculated C–O bond cleavage in  $[R_F$ –COO] $\bullet^2$  structures indeed occurred at the first ether linkage counted from –COO $^-$ , the cleaved C–O bond was not the "significantly weaker one" as calculated in the original  $R_F$ –COO $^-$  (e.g., **Figure 5c** versus **4n**). This discrepancy could be due to the addition of the extra electron, which altered the bonding structure of PFECA anions. More importantly, the calculation shows that C–O bond cleavage can be a major pathway for PFECA degradation by  $e_{aq}$ . The previously elucidated cleavage of weak C–F bonds<sup>40</sup> was also observed both from branched PFECAs (with very weak tertiary C–F bonds) and from the linear structure BI CF3–O–CF2–COO $^-$  where the  $\alpha$ -position C–F BDE is relatively high (112 kcal mol $^{-1}$ ). These results suggest that C–F bond cleavage can be another degradation pathway, even if the inclusion of ether oxygen atoms makes many C–F bonds more recalcitrant than those in full-carbon-chain PFCAs.

*PFECA Degradation Product Analysis.* The above theoretical calculations have indicated the possibility of C–F and C–O bond cleavage. Based on our previous study, the decarboxylation-hydroxylation-HF elimination-hydrolysis (*DHEH*) is another major degradation pathway for structures with the fluoroalkyl moiety directly linked with –COO<sup>-</sup>.<sup>40</sup> Hence, we hypothesized that the degradation of PFECAs takes place via at least three pathways: (i) cleavage of weak C–F bonds and the formation of C–H bonds (i.e., H/F exchange), (ii) *DHEH*, and (iii) the characteristic

cleavage of ether C-O bonds. To detect the transformation products (TPs) and confirm the degradation pathways, we used both targeted analysis with triple quadruple mass spectrometry and suspect screening with high-resolution mass spectrometry data (all results collected in SI Tables S1-S9). A series of TPs was detected, well supporting all three proposed degradation pathways. The overall TP detection and corresponding degradation pathways from the longest PFECA in each of the four structure categories are discussed below (Figure 6, and Schemes 1 and 2). The reaction schemes proposed for individual PFECAs are provided in SI Schemes S1-S10.

229

230

231

232

233

234

235

236

237

238

239

240

241

242

243

244

245

246

247

248

249

250

As shown in Figure 6a, the degradation of A3 HFPO-TeA generated A2 HFPO-TrA and A1 HFPO-DA daughter products. The maximum concentration of A2 (7.9  $\mu$ M) and A1 (3.7  $\mu$ M) were detected at 8 h and 12 h, respectively. We attribute this transformation to the cleavage of the first C-O bond counted from the terminal -COO-. The two fragments reacted with H<sub>2</sub>O to form two perfluorinated alcohols, which were not stable and subject to HF elimination to acyl fluoride. 42, <sup>43</sup> The subsequent hydrolysis generated the carboxylic acid, resulting in the net conversion from  $R_F$ -CF<sub>2</sub>OH into  $R_F$ -COO<sup>-</sup> and two F<sup>-</sup> ions. The C-O cleavage on the first ether linkage counted from -COO shortens HFPO-TeA into HFPO-TrA, then into HFPO-DA, which can be further degraded into CF<sub>3</sub>CF<sub>2</sub>-COO<sup>-</sup> via another C-O cleavage (**Scheme 1**). Each round of C-O cleavage also generated the same product CF<sub>3</sub>CF(OH)-COO<sup>-</sup>, which underwent further HF elimination into CF<sub>3</sub>-CO-COO<sup>-</sup> (trifluoropyruvate, TFPy), as structures with F and OH on the same carbon (e.g., FCH<sub>2</sub>OH) are generally unstable.<sup>44</sup> We confirmed the formation of TFPy during the degradation of HFPO-DA with IC detection (SI Figure S8). Like CF<sub>3</sub>-COO<sup>-</sup> (trifluoroacetic acid, TFA), the pure TFPy also showed near-complete defluorination (SI Figure S9), and TFA is a possible degradation intermediate (SI Figure S10). Although TFA was not detected in our samples from HFPO-DA degradation, we have elucidated that TFA can be generated from both CF<sub>3</sub>CF<sub>2</sub>–COO<sup>-</sup> and TFPy, and then completely mineralized via the *DHEH* pathway (**Scheme 1b**).<sup>40</sup>

Suspect screening using the high-resolution MS data identified a series of H/F exchange products from the HFPO oligomer acids. Based on the calculation results, we assign the C–H bonds to the branched carbons (particularly the α-position branched carbon) where weak tertiary C–F bonds are located (**Figure 6b** and **Scheme 1a**). We also observed products missing one or more –CF<sub>3</sub> groups (i.e., H/CF<sub>3</sub> exchange). By comparing the results with those for linear PFECAs, such TP structures missing –CF<sub>3</sub> groups are specific for branched PFECAs. Therefore, we interpret the transformation pathway to be the cleavage of the branching –CF<sub>3</sub> rather than the terminal –CF<sub>3</sub>. In addition, the degradation products and reaction schemes from pure HFPO-TrA and HFPO-DA (**SI Tables S1–S2** and **Schemes S1–S2**) further corroborate the mechanistic insights obtained from HFPO-TeA degradation.

For the degradation of *B3* (CF<sub>3</sub>–O–CF<sub>2</sub>CF<sub>2</sub>CF<sub>2</sub>–COO<sup>-</sup>), the C–O bond cleavage mechanism was confirmed by the detection of OOC–CF<sub>2</sub>CF<sub>2</sub>–COO<sup>-</sup> (Figure 6c and Scheme 2a). The head CF<sub>3</sub>– group was thus believed to be fully defluorinated via the formation of unstable CF<sub>3</sub>–OH. The *DHEH* mechanism was also confirmed by the generation of *B2* CF<sub>3</sub>–O–CF<sub>2</sub>CF<sub>2</sub>–COO<sup>-</sup>. The HRMS detection of two products with one and two H/F exchanges on the parent compound (most probably at the α-position) is not surprising (Figure 6d).

The degradation of the two multi-ether linear PFECAs C2 and D2 also followed the three reaction pathways, which are supported by the TPs identified (**Figures 6e-6h**). Although the C-F BDEs of the  $\alpha$ -position  $-CF_2$ — in these structures are higher than in full-carbon-chain PFCAs

(**Figure 4g** versus **4f**), the H/F-exchanged TPs were detected, thus corroborating the spontaneous C–F bond stretching by theoretical calculations (**Figure 5a**).

Additionally, the C-O bond cleavage in B1 (also in category C and D structures that contain  $-O-CF_2-COO^-$ ) was supposed to generate  $HO-CF_2-COO^-$ , which should further decompose into oxalate ( $^-OOC-COO^-$ ). IC detection confirmed the formation of oxalate (SI Figure S11), thus further consolidating this C-O bond cleavage mechanism.

Overall Mechanistic Insights into Reductive PFECA Degradation. Based on the degradation kinetics, theoretical calculation, and TP analysis, we have confirmed that the PFECAs have three pathways for the reductive degradation by  $e_{aq}^-$ : (1) ether C-O bond cleavage, (2) C-C bond cleavage, including the decarboxylation step of *DHEH* and the cleavage of -CF<sub>3</sub> from branched PFECAs, and (3) direct C-F bond cleavage followed by H/F exchange. Here we categorize the first two as *indirect* pathways for defluorination, and the third one as a *direct* pathway for defluorination. It is worth noting here that all three independent pathways are enabled upon the PFECAs interacting with  $e_{aq}^-$ . First, control experiments with UV irradiation without adding sulfite showed very slow and limited degradation (SI Figure S12). Second, spontaneous C-O bond cleavage was observed after the PFECA anion received an extra electron (Figure 5). Third, the generation of  $e_{aq}^-$  from sulfite has been confirmed by spectroscopic observations,  $^{45,46}$  and other chemicals such as iodide  $^{47}$  and indole  $^{48}$  have also been used as the source of  $e_{aq}^-$  and achieved similar results for PFOA defluorination.

The cleavage of the C–O or C–C bond in PFECAs will generate perfluoroalcohols, which will undergo HF elimination and the following hydrolysis to yield two F<sup>-</sup> and the corresponding carboxylic acids. This mechanism has been collectively supported by (1) the decay of HFPO and

TFEO oligomer acids into shorter analogs (**Figures 6a, 6e,** and **6g,** supporting C–O cleavage) and the decay of B3 into B2 (**Figure 6c,** supporting C–C cleavage), (2) the generation of  $^{-}$ OOC–CF<sub>2</sub>CF<sub>2</sub>CF<sub>2</sub>–COO $^{-}$  from B3 (CF<sub>3</sub>–O–CF<sub>2</sub>CF<sub>2</sub>CF<sub>2</sub>–COO $^{-}$ ) and the generation of  $^{-}$ OOC–COO $^{-}$  from  $R_F$ –O–CF<sub>2</sub>–COO $^{-}$  structures, and most importantly (3) the high deF% of linear PFECAs with short oxygen-segregated fluorocarbon moieties. Results in **Figures 3d, 3f,** and **3h** show the clear trend that PFECAs containing longer fluorocarbon moieties (rather than the longer molecule) yielded lower deF%. Since the perfluoroalcohol decomposition can only ensure the liberation of two F $^{-}$  ions, if this step yields a full-carbon-chain PFCA containing two or more fluorocarbons, relatively easy H/F exchange on the  $\alpha$ -position will occur, yielding  $R_F$ –CH<sub>2</sub>–COO $^{-}$ . As previously elucidated, the reductive defluorination of this product is very sluggish, especially when the  $R_F$  moiety is short (i.e., lack of weak C–F bonds).  $^{40}$ 

Among all PFECAs, B1 (CF<sub>3</sub>–O–CF<sub>2</sub>–COO<sup>-</sup>) allowed an outstanding deF% at 91% because either C–O cleavage or decarboxylation will trigger the perfluoroalcohol decomposition mechanism to liberate all five F<sup>-</sup> ions from the two oxygen-segregated single fluorocarbons. We hypothesized that the incomplete defluorination was attributed to the minor chance of H/F exchange on the  $\alpha$ -position (**Figure 5a**). To verify this hypothesis, we examined the degradation of polyfluorinated CF<sub>3</sub>–O–CH<sub>2</sub>–COO<sup>-</sup> under the same reaction condition (**Figure 7**). As expected, the –CH<sub>2</sub>– group at the  $\alpha$ -position leads to a high recalcitrance in comparison with B1 (**Figure 3c** and **3d**). However, to our surprise, the degradation at 24 h (30%) was much higher than the full-carbon-chain counterpart CF<sub>3</sub>CH<sub>2</sub>–COO<sup>-</sup> (< 2%). <sup>40</sup> The overall deF% of 28% indicates a near-complete defluorination of the decayed 30% fraction of the parent compound, and the time profiles of parent compound decay and defluorination are highly symmetric. These results support the degradation mechanism of C–O bond cleavage rather than a stepwise H/F exchange. Therefore,

C-O bond cleavage can still occur in a *poly*fluorinated ether structure with a hydrocarbon moiety segregating the -COO<sup>-</sup> group from the fluorinated moiety. The rate is faster than in a *poly*fluorinated full-carbon-chain structure but slower than in a *per*fluorinated ether structure.

317

318

319

320

321

322

323

324

325

326

327

328

329

330

331

332

333

334

335

336

337

338

339

For comparison, under the same reaction condition, the deF% for the full-carbon CF<sub>3</sub>CF<sub>2</sub>-COO<sup>-</sup> was 53%. 40 In our previous study, by assuming that CF<sub>3</sub>CF<sub>2</sub>-COO<sup>-</sup> will take either H/F exchange (forming the highly recalcitrant CF<sub>3</sub>CH<sub>2</sub>-COO<sup>-</sup> with negligible further degradation, thus the overall deF% is 40%) or DHEH (leading to 100% defluorination via forming CF<sub>3</sub>-COO<sup>-</sup>), we estimated that the chance for CF<sub>3</sub>CF<sub>2</sub>-COO<sup>-</sup> taking H/F exchange versus *DHEH* is 75% versus 25%. 40 Similarly, if all **B1** CF<sub>3</sub>-O-CF<sub>2</sub>-COO<sup>-</sup> first undergoes C-O or C-C bond cleavage, 100% defluorination would be achieved. If all B1 first undergoes H/F exchange to yield CF<sub>3</sub>-O-CH<sub>2</sub>-COO<sup>-</sup> (deF% = 40% at this step), which then undergoes slow degradation for up to 30%, this would result in  $40\% + 60\% \times 30\% = 58\%$  defluorination. Hence, to yield an overall defluorination of 91% through the two competing pathways, the probability for **B1** to take H/F exchange is only 21%. This significantly lowered probability of H/F exchange from 75% to 21% should be attributed to the elevated  $\alpha$ -position C-F BDE in the  $R_F$ -O-CF<sub>2</sub>-COO<sup>-</sup> structures (Figures 4a, 4g, and 4h). This mechanistic insight also explains the low deF\% for B2 CF<sub>3</sub>-O-CF<sub>2</sub>CF<sub>2</sub>-COO<sup>-</sup> and **B3** CF<sub>3</sub>-O-CF<sub>2</sub>CF<sub>2</sub>CF<sub>2</sub>-COO<sup>-</sup> as the lower α-position C-F BDEs (Figures 4b and 4c) enabled easier H/F exchange. In Figure 3, the parent compound decay of B2 and **B3** were faster than all  $R_F$ -O-CF<sub>2</sub>-COO<sup>-</sup> compounds. The formation of -CH<sub>2</sub>- at the  $\alpha$ position significantly slowed down the further degradation. In contrast, all PFECAs that allowed higher deF% than PFCAs (~55%)<sup>40</sup> contain only short (C1 or C2) fluorocarbon moieties, which suppress the direct defluorination via H/F exchange (unfavorable pathway, typically breaking weak C-F bonds) and enhance the *indirect* defluorination via C-O or C-C bond cleavage

(favorable pathway, breaking all C-F bonds on the carbon bearing the -OH, regardless of the BDEs).

The above mechanistic insights also explain the degradation pattern of branched PFECAs. The branching –CF<sub>3</sub> generates distinctly weak tertiary C–F bonds, especially at the α-position (Figure 4i and SI Figure S2). As shown in Figures 5b and 6b, these structures have a high tendency to undergo H/F exchange. The following cleavage of the branching –CF<sub>3</sub> leads to the formation of –CH<sub>2</sub>– at the α-position, thus retarding further degradation. The longest structure A3 has three tertiary C–F bonds; thus the parent A3 and the C–O cleavage products A2 and A1 all have a high chance for the unfavorable H/F exchange. Therefore, A3 showed the lowest deF% among the three branched PFECAs. From the HRMS data for all PFECAs (SI Tables S1–S9), in general, the TPs with one H/F exchange increased at the beginning of the reaction, then slowly decreased. In contrast, the two H/F exchange TPs slowly accumulated throughout the reaction, indicating high recalcitrance. In comparison to linear PFECAs and full-carbon-chain PFCAs, the slower parent compound decay of branched PFECAs is probably attributed to the kinetic hindrance by the branching –CF<sub>3</sub>.

We note that earlier studies by Bao *et al.*<sup>38, 39</sup> on the degradation of HFPO oligomer acids (*A1*, *A2*, and *A3*) observed significantly faster parent compound decay and higher deF% than our observations. In comparison to our reaction settings (one UV lamp for a 600-mL solution, pH 9.5, and 10 mM sulfite), Bao *et al.* used considerably more favorable conditions, including intense UV irradiation (sixteen similar UV lamps for a 45-mL solution), tripled basicity (pH 10), and doubled sulfite concentration (20 mM). Because the duplication of 20 mM sulfite at pH 10 in our photoreactors (one UV lamp for a 600-mL solution) achieved limited improvements on deF% (SI Figure S13), the significantly higher defluorination observed by Bao *et al.*<sup>38, 39</sup> should be attributed

to the higher intensity of the 254-nm UV irradiation. Nonetheless, by comparing all PFECA compounds, we have identified new structural features allowing much deeper defluorination than HFPO oligomers. We expect that further enhanced degradation of PFECA structures can be achieved under energy-efficient reaction conditions, which are under optimization in our lab.

363

364

365

366

367

368

369

370

371

372

373

374

375

376

377

378

379

380

381

382

383

384

385

Implications for Fluorochemical Design and Environmental Remediation. As seen from the diverse PFECA structures involved in this study, the design of PFECA is highly flexible as multiple fluorinated building blocks can be integrated into the molecule in various sequences. Although the design rationale of individual PFECAs (e.g., branched vs. linear, and the length of oxygen-segregated fluorocarbon moieties) and their targeted properties for specific industrial applications remain largely unknown to the environmental chemistry community, we are able to identify critical molecular features that can lead to enhanced PFECA degradation using reductive approaches. UV irradiation (on sulfite, iodide, indole, or hydroxyl radical scavengers), 46-49 plasma treatment, <sup>34</sup> and high-energy irradiation <sup>33</sup> all involve  $e_{aq}$  as a primary reactive species. In general, the switch from full-carbon-chain PFCAs to PFECAs has indeed brought in unique advantages that enable deeper defluorination, including (1) spontaneous defluorination from alcohol intermediates upon C–O cleavage and (2) suppressed H/F exchange due to the strong C–F bonds. To minimize the incomplete defluorination caused by the conversion into recalcitrant products (e.g., with -CH<sub>2</sub>- separating the fluoroalkyl moiety and the -COO<sup>-</sup>), a desirable structural feature is  $R_F$ -O-CF<sub>2</sub>-COO<sup>-</sup>. In other words, the last building block of the PFECA molecule can be a tetrafluoroethylene oxide; after the epoxide ring opens, the alcohol product  $R_F$ —O-CF<sub>2</sub>CF<sub>2</sub>OH will transform to  $R_F$ -O-CF<sub>2</sub>-COO<sup>-</sup>. As elucidated in earlier sections, the relatively high BDE of the α-position C-F favors *indirect* defluorination through C-O cleavage and decarboxylation. The other desirable structural feature is to limit the length of other fluorocarbon moieties segregated by ether oxygen atoms. If the chain length is C1 (either CF<sub>3</sub>–O– or –O–CF<sub>2</sub>–O–), the C–O cleavage is expected to provide complete defluorination of that fluorocarbon moiety. This prediction, which is based on model PFECAs studied in this work, can be further examined when chemicals containing –O–CF<sub>2</sub>–O– moieties (e.g., CF<sub>3</sub>–(O–CF<sub>2</sub>)<sub>n</sub>–O–CF<sub>2</sub>–COO<sup>–</sup>, n = 1 to 3)<sup>24, 27</sup> become available for experimental tests. Because the oxygen atoms substantially elevate C–F BDEs (**Figure 4**), direct H/F exchange on C1 or C2 fluorocarbon moieties (not linked with –COO<sup>–</sup>) is less likely. However, for C2 fluorocarbon moieties (e.g., –O–CF<sub>2</sub>CF<sub>2</sub>–O–), the formation of –O–CF<sub>2</sub>–COO<sup>–</sup> will still induce a low probability of H/F exchange.

On the other hand, the mechanistic insights from this study will guide the development of PFECA degradation technologies. In particular, if the *direct* defluorination cannot be fully avoided, effective degradation of the recalcitrant *poly*fluorinated products will be necessary to ensure a deep or complete defluorination. While we observed poor defluorination from the branched PFECAs that contain very weak tertiary C–F bonds and a long C3 fluorocarbon moiety, studies by Bao *et al.*<sup>38, 39</sup> have achieved deep defluorination of those structures by applying high UV intensity. Therefore, coordinated efforts from both fluorochemical design (e.g., developing PFECAs with high degradability) and environmental remediation (e.g., optimizing the consumption of energy and chemicals) can be expected to transform the development, use, and treatment of fluorinated chemicals with minimal adverse impact to the environment.

### 404 ASSOCIATED CONTENT

# 405 **Supporting Information**

- The Supporting Information is available free of charge on the ACS Publications website at DOI:
- 407 10.1021/acs.est.xxxxxxx.
- Additional tables, figures, discussions, and detailed experimental procedures.

## **409 AUTHOR INFORMATION**

- 410 Corresponding Author
- \*(J.L.) E-mail: jyliu@engr.ucr.edu; jinyong.liu101@gmail.com.
- 412 Notes
- The authors declare no competing financial interest.

# 414 ACKNOWLEDGEMENTS

- 415 Financial support was provided by the UCR Initial Complement for J.L., UCR Collaborative Seed
- 416 Grant for J.L., B.M.W., L.X., and H.K.; the National Science Foundation (CHE-1709719 for J.L.
- and CHE-1709286 for Y.M. and Y.Y.), and the Strategic Environmental Research and
- Development Program (ER-1289 for J.L., M.B., and B.M.W). M.B. also received a scholarship
- from the UCR Water SENSE Integrative Graduate Education and Research Traineeship (IGERT)
- supported by NSF. UCR undergraduate researchers Andrew Dalmacio, Duy Dao, Maggy Harake,
- Vivian Ngo, and Wenxiaoshan Sui provided technical assistance on photochemical reactions. We
- also thank Dr. Mark Strynar for kindly providing compound *B1*.

Table 1. Overall Defluorination Percentages of PFECAs after 48 Hours of Reaction.<sup>a</sup>

424

425

426

427

428

429

Entry	Structure	n	deF%
A. Branched (HFPO oligomers)			
A1	F, F P	1	$44.9 \pm 5.3$
A2	F O O	2	$36.5 \pm 2.9$
A3	F F F In U	3	$30.8 \pm 4.2$
	F · · F F		

# **B.** Mono-ether with head CF<sub>3</sub>O-

B1
 
$$F$$
 $F$ 
 $F$ 

# *C.* TFEO oligomers with head CF<sub>3</sub>O-

# **D.** TFEO oligomers with head $C_4F_9O$ -

# E. Full-carbon-chain PFCAsb

E1 
$$\bigcirc$$
 1 98.2 ± 5.0  $\bigcirc$  2-10 54.5 ± 3.5

<sup>a</sup>Reaction condition: PFAS (0.025 mM), Na<sub>2</sub>SO<sub>3</sub> (10 mM), carbonate buffer (5 mM), 254 nm irradiation (a 18 W low-pressure Hg lamp for 600 mL solution) at pH 9.5 and 20°C.

<sup>b</sup>Data from Ref. 40 for comparison. The average and standard deviation of the deF% value for n=2-10 is based on 27 data points (nine PFCA structures with triplicates).

Perfluoro(2-methyl-3-oxahexanoate) (GenX, CAS No. 62037-80-3)

3H-perfluoro-3-[(3-methoxy-propoxy) propionic acid)]

(ADONA, CAS No. 958445-44-8)

Perfluoro[(2-ethyloxy-ethoxy)acetic acid] (EEA, CAS No. 908020-52-0)

430 431

432

**Figure 1.** Examples of commercial perfluorinated (GenX and EEA) and polyfluorinated (ADONA) ether carboxylic acids detected in the environment.

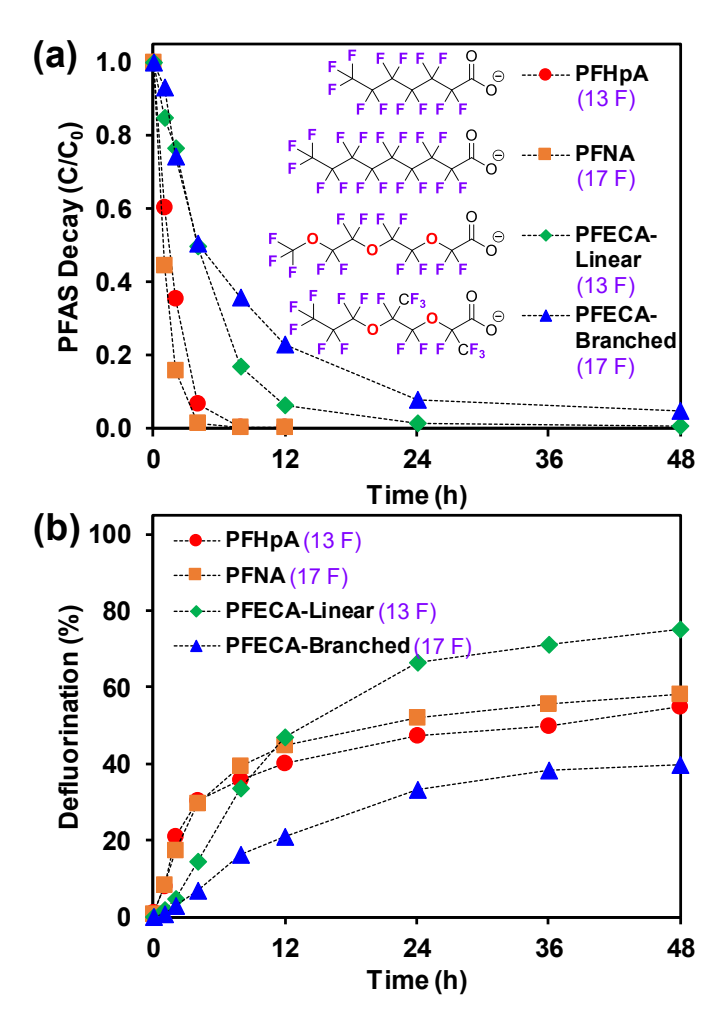


**Figure 2.** Time profiles for **(a)** parent compound decay and **(b)** defluorination percentages for two full-carbon-chain PFCAs with 13 and 17 F atoms, a linear PFECA with 13 F atoms, and a branched PFECA with 17 F atoms. Reaction conditions: PFAS (0.025 mM), Na<sub>2</sub>SO<sub>3</sub> (10 mM), carbonate buffer (5 mM), 254 nm irradiation (a 18 W low-pressure Hg lamp for 600 mL solution) at pH 9.5 and 20°C.

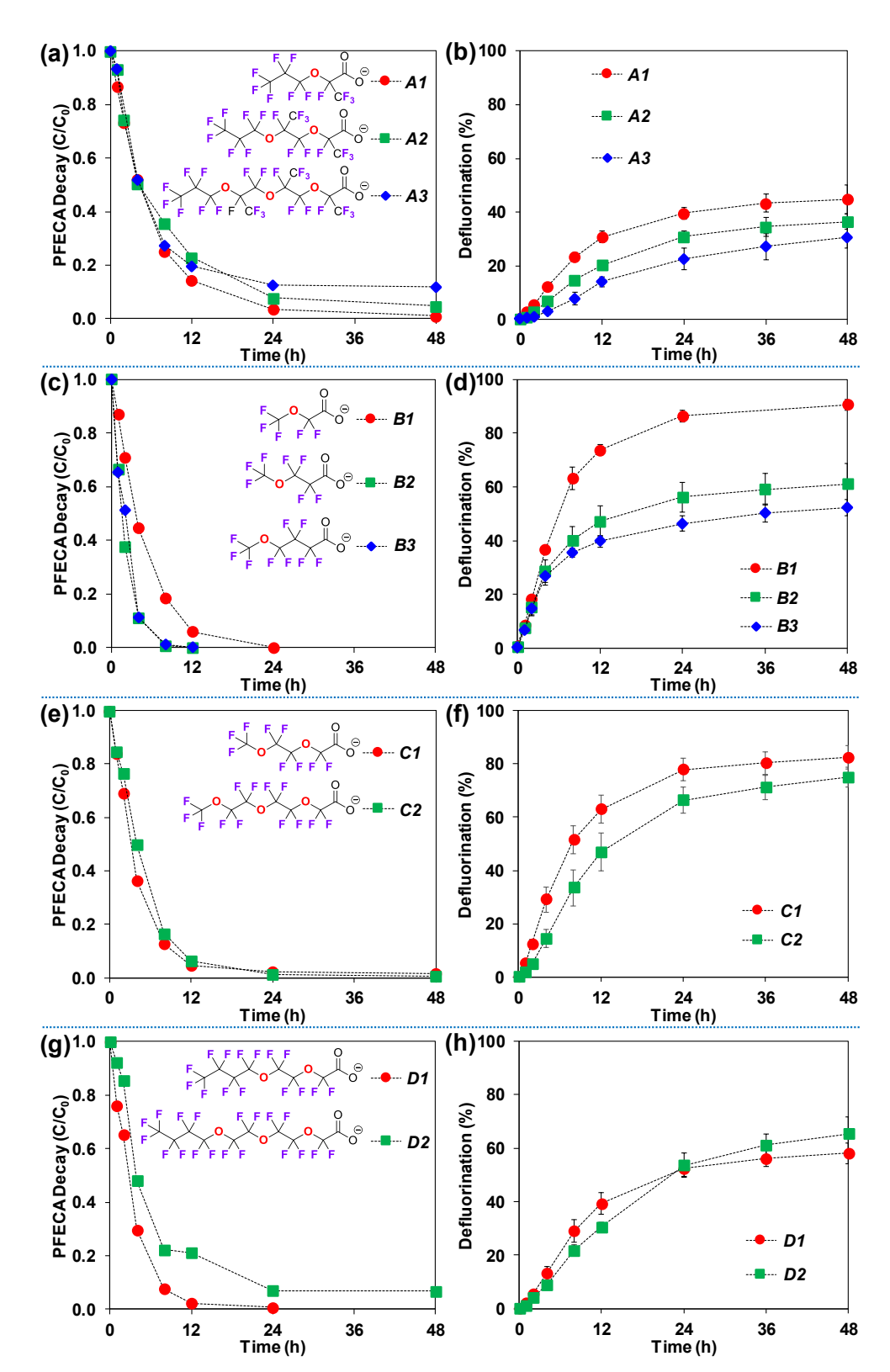


**Figure 3.** Time profiles of parent compound decay and defluorination for the four PFECA structure categories. Reaction conditions are described in the title of **Figure 2**.

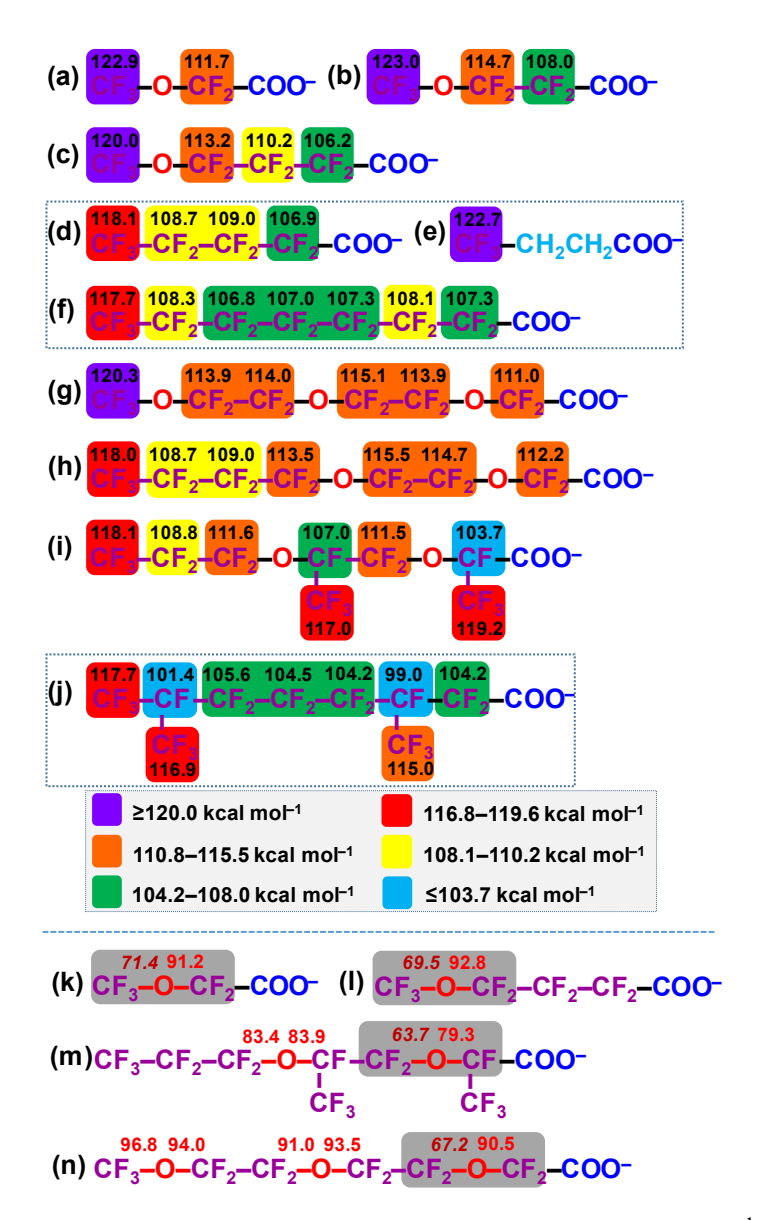


**Figure 4.** Calculated C-F BDEs (**a** to **j**) and C-O BDEs (**k** to **n**) (in kcal mol<sup>-1</sup>) of selected PFASs at the B3LYP-D3(BJ)/6-311+G(2d,2p) level of theory. Results for all PFECA structures are collected in **SI Figures S2–S5**. Data for (**d**)–(**f**) and (**j**) are from Ref 40 and Ref 41, respectively.

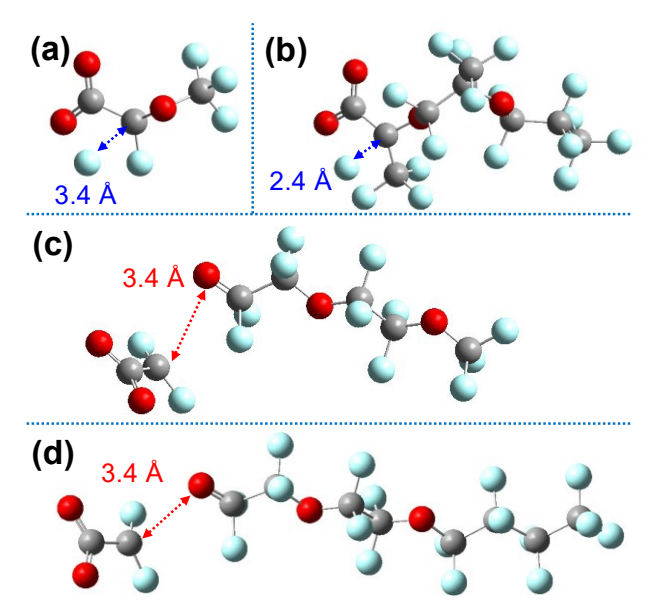


**Figure 5.** Geometry-optimized structure of the adducts of PFECA anions with an  $e_{aq}^-$  (PFECA $\bullet^{2-}$ ) at the B3LYP-D3(BJ)/6- 311+G(2d,2p) level of theory, showing the stretching of C-F (blue) and C-O (red) bonds. Results for all PFECA structures are collected in **SI Figures S6–S7**.

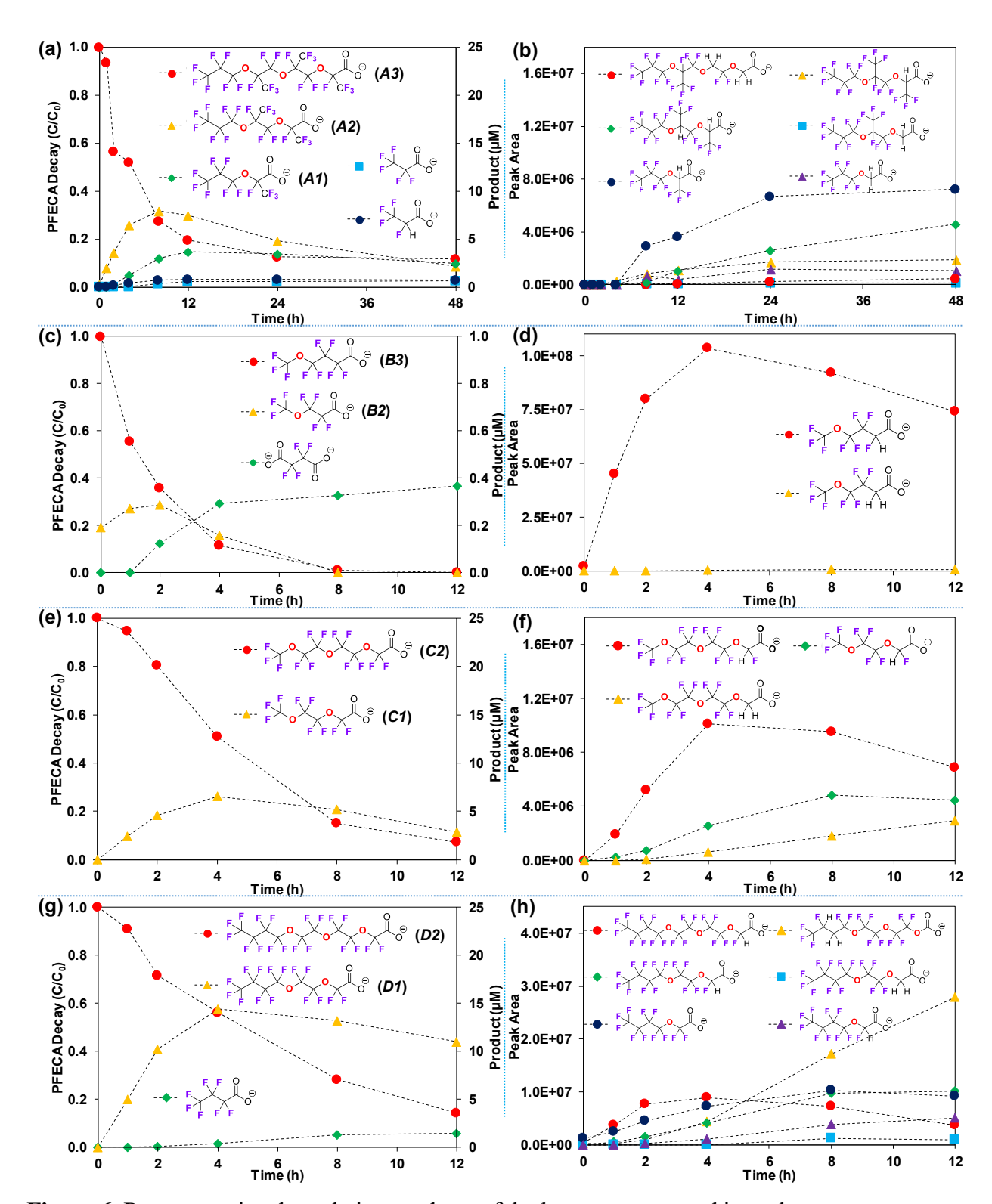


**Figure 6.** Representative degradation products of the longest compound in each structure category (A3, B2, C2, and D2,  $C_0 = 25 \mu M$ ). Reaction conditions are described in the title of **Figure 2**. For each structure, quantified products with standard compounds are shown in the left panel, and species without standard compounds are presented in peak areas in the right panel. All detected species are listed in **SI Tables S1–S9**.

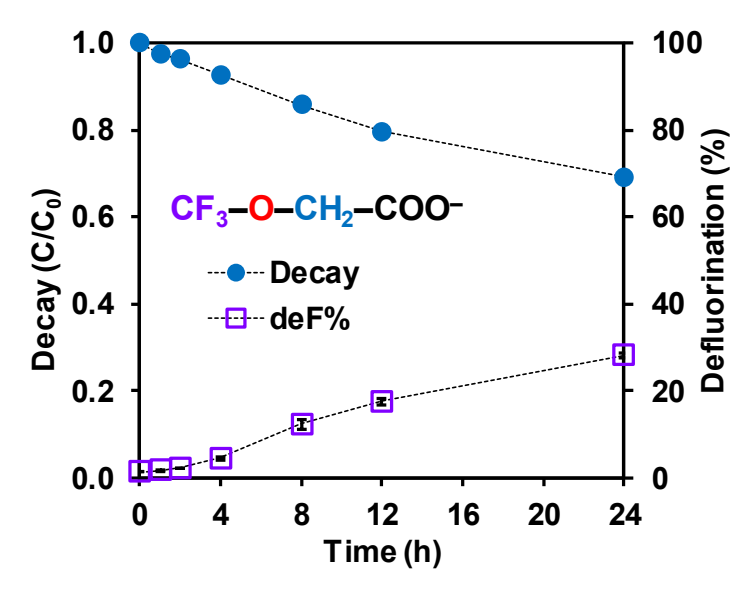
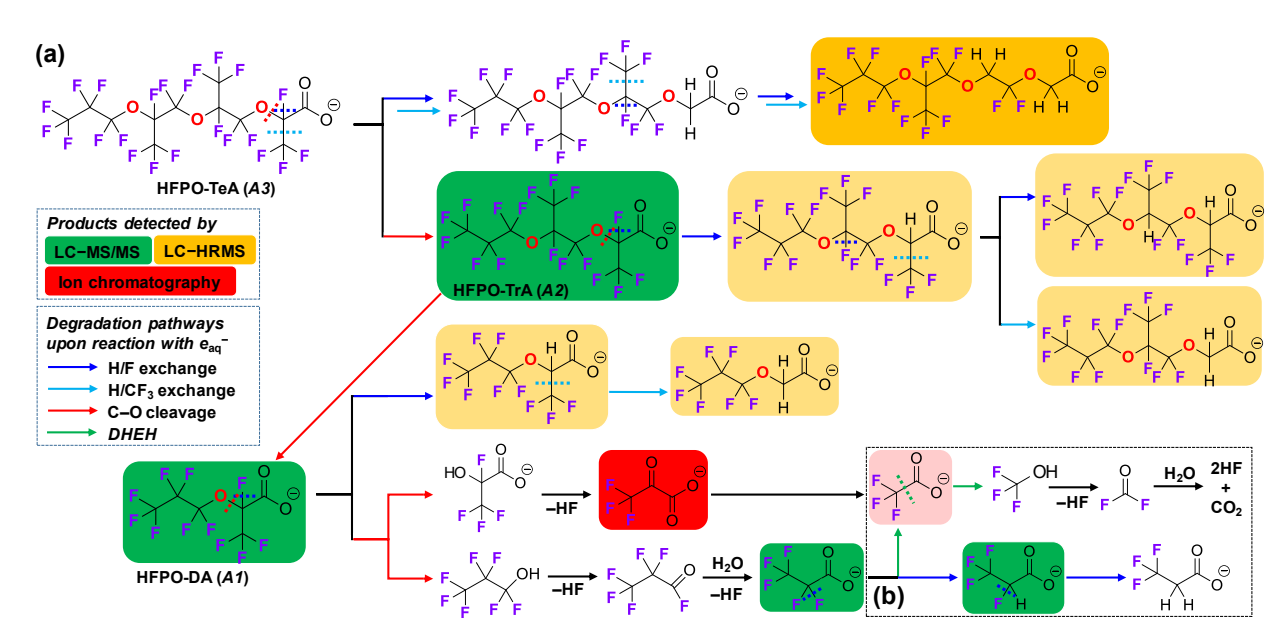
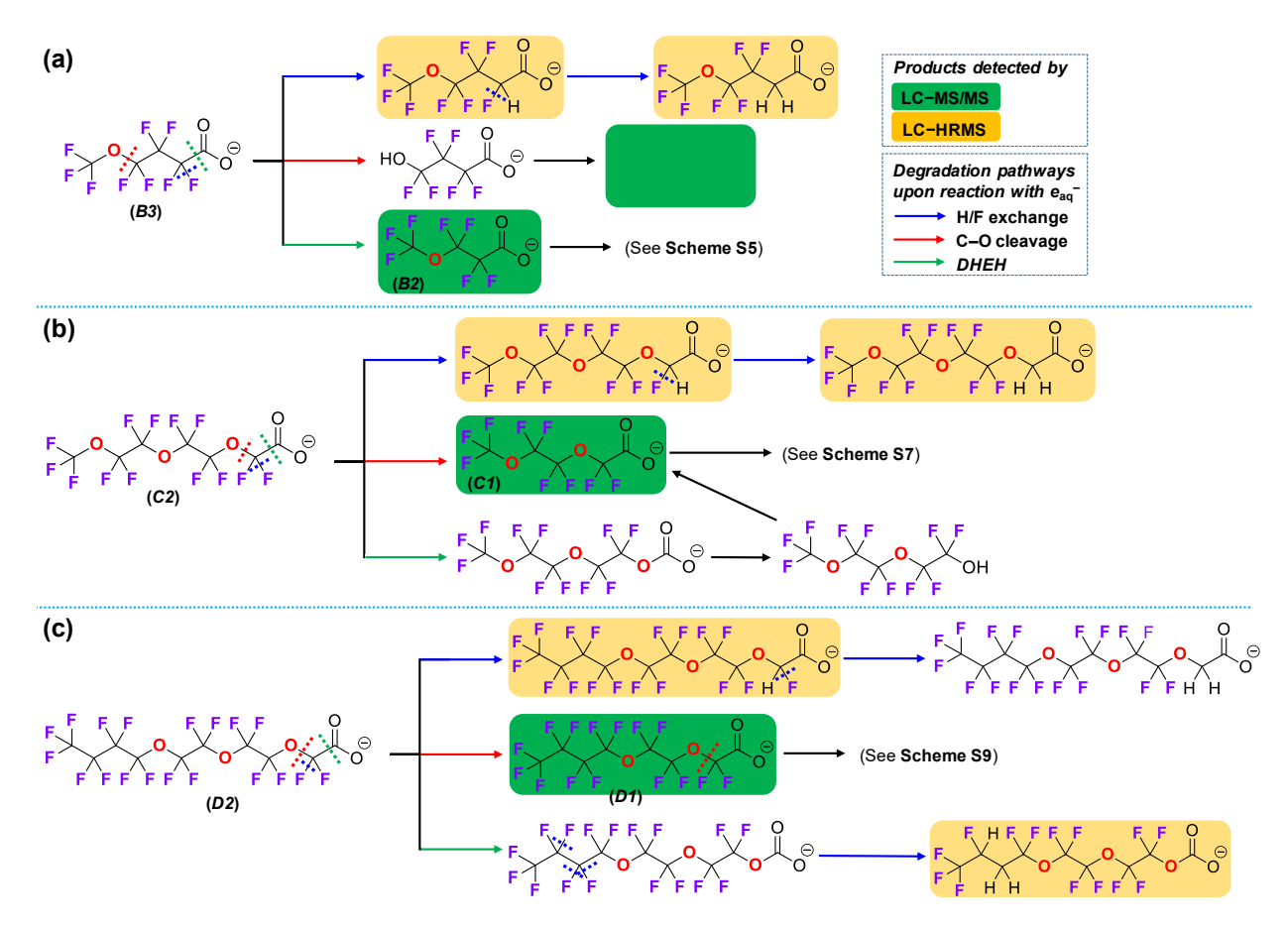


**Figure 7.** Time profiles of parent compound decay and defluorination for polyfluorinated CF<sub>3</sub>–O–CH<sub>2</sub>–COO<sup>–</sup> under the same reaction condition for all other PFECAs (described in the title of **Figure 2**).



**Scheme 1.** Degradation pathways for **(a)** HFPO oligomer acids starting from the longest compound A3 and **(b)** the daughter product PFPrA. Detected transformation products are highlighted.



Scheme 2. Degradation pathways for the three PFECA structure categories starting from the longest compound (a) B3, (b) C2, and (c) D2. Detected transformation products are highlighted.

## References

- 469 1. Banks, R. E.; Smart, B. E.; Tatlow, J., Organofluorine chemistry: principles and commercial
- 470 *applications*. Springer Science & Business Media: 2013.
- 471 2. Wang, Z.; DeWitt, J. C.; Higgins, C. P.; Cousins, I. T., A never-ending story of per-and
- 472 polyfluoroalkyl substances (PFASs)? Environ. Sci. Technol. 2017, 51, (5), 2508-2518.
- 473 3. Buck, R. C.; Franklin, J.; Berger, U.; Conder, J. M.; Cousins, I. T.; De Voogt, P.; Jensen, A. A.;
- 474 Kannan, K.; Mabury, S. A.; van Leeuwen, S. P., Perfluoroalkyl and polyfluoroalkyl substances in the
- 475 environment: terminology, classification, and origins. *Integrated environmental assessment and*
- 476 management **2011**, 7, (4), 513-541.
- 4. Meshri, D. T., The modern inorganic fluorochemical industry. *Journal of fluorine chemistry* **1986,**
- 478 33, (1-4), 195-226.
- 479 5. Xiao, F., Emerging poly-and perfluoroalkyl substances in the aquatic environment: a review of
- 480 current literature. *Water research* **2017**, *124*, 482-495.
- 481 6. Liu, J.; Avendaño, S. M., Microbial degradation of polyfluoroalkyl chemicals in the environment:
- a review. *Environment International* **2013,** *61*, 98-114.
- 483 7. Kelly, B. C.; Ikonomou, M. G.; Blair, J. D.; Surridge, B.; Hoover, D.; Grace, R.; Gobas, F. A.,
- 484 Perfluoroalkyl contaminants in an Arctic marine food web: trophic magnification and wildlife exposure.
- 485 Environmental science & technology **2009**, *43*, (11), 4037-4043.
- 486 8. Agency, U. S. E. P., Revisions to the Unregulated Contaminant Monitoring Regulation (UCMR 3)
- 487 for Public Water Systems. *Federal Register* **2012,** *77,* (85), 26071-26101.
- 488 9. Agency, U. S. E. P., Lifetime Health Advisories and Health Effects Support Documents for
- 489 Perfluorooctanoic Acid and Perfluorooctane Sulfonate Federal Register 2016, 81, (101), 33250-33251.
- 490 10. COMMISSION REGULATION (EU) 2017/1000 of 13 June 2017 amending Annex XVII to Regulation
- 491 (EC) No 1907/2006 of the European Parliament and of the Council concerning the Registration,
- 492 Evaluation, Authorisation and Restriction of Chemicals (REACH) as regards perfluorooctanoic acid
- 493 (PFOA), its salts and PFOA-related substances. . Official Journal of the European Union 2017, 14.6.2017, L
- 494 150/14-L 150/18.
- 495 11. Post, G. B.; Gleason, J. A.; Cooper, K. R., Key scientific issues in developing drinking water
- 496 guidelines for perfluoroalkyl acids: Contaminants of emerging concern. PLoS biology 2017, 15, (12),
- 497 e2002855.
- 498 12. U.S. EPA. 2010/15 PFOA Stewardship Program. . https://www.epa.gov/assessing-and-managing-
- 499 chemicals-under-tsca/risk-management-and-polyfluoroalkyl-substances-pfass#tab-3.
- 500 13. Wang, J.; Pan, Y.; Cui, Q.; Yao, B.; Wang, J.; Dai, J., Penetration of PFASs across the blood
- 501 cerebrospinal fluid barrier and its determinants in humans. Environmental science & technology 2018,
- 502 *52*, (22), 13553-13561.
- 503 14. Rappazzo, K.; Coffman, E.; Hines, E., Exposure to perfluorinated alkyl substances and health
- outcomes in children: a systematic review of the epidemiologic literature. *International journal of*
- environmental research and public health **2017**, *14*, (7), 691.
- 506 15. Sustainability | GenX | Teflon coatings for Industrial Bakery Solutions.,
- 507 https://www.chemours.com/Industrial Bakery Solutions/en GB/sustainability/dibs genx.html.
- 508 16. Conley, J. M.; Lambright, C. S.; Evans, N.; Strynar, M. J.; McCord, J.; McIntyre, B. S.; Travlos, G. S.;
- 509 Cardon, M. C.; Medlock-Kakaley, E.; Hartig, P. C., Adverse Maternal, Fetal, and Postnatal Effects of
- 510 Hexafluoropropylene Oxide Dimer Acid (GenX) from Oral Gestational Exposure in Sprague-Dawley Rats.
- 511 *Environmental health perspectives* **2019,** *127,* (3), 037008.
- 512 17. Sheng, N.; Pan, Y.; Guo, Y.; Sun, Y.; Dai, J., Hepatotoxic effects of hexafluoropropylene oxide
- trimer acid (HFPO-TA), a novel perfluorooctanoic acid (PFOA) alternative, on mice. Environmental
- *science & technology* **2018,** *52,* (14), 8005-8015.

- 515 18. Cui, Q.; Pan, Y.; Zhang, H.; Sheng, N.; Wang, J.; Guo, Y.; Dai, J., Occurrence and tissue distribution
- of novel perfluoroether carboxylic and sulfonic acids and legacy per/polyfluoroalkyl substances in black-
- 517 spotted frog (Pelophylax nigromaculatus). Environmental science & technology 2018, 52, (3), 982-990.
- 518 19. Sheng, N.; Cui, R.; Wang, J.; Guo, Y.; Wang, J.; Dai, J., Cytotoxicity of novel fluorinated
- alternatives to long-chain perfluoroalkyl substances to human liver cell line and their binding capacity to
- 520 human liver fatty acid binding protein. Archives of toxicology 2018, 92, (1), 359-369.
- 521 20. Wang, Z.; Cousins, I. T.; Scheringer, M.; Hungerbühler, K., Fluorinated alternatives to long-chain
- 522 perfluoroalkyl carboxylic acids (PFCAs), perfluoroalkane sulfonic acids (PFSAs) and their potential
- 523 precursors. *Environment international* **2013**, *60*, 242-248.
- 524 21. Strynar, M.; Dagnino, S.; McMahen, R.; Liang, S.; Lindstrom, A.; Andersen, E.; McMillan, L.;
- 525 Thurman, M.; Ferrer, I.; Ball, C., Identification of novel perfluoroalkyl ether carboxylic acids (PFECAs) and
- sulfonic acids (PFESAs) in natural waters using accurate mass time-of-flight mass spectrometry (TOFMS).
- 527 Environmental science & technology **2015**, 49, (19), 11622-11630.
- 528 22. Pan, Y.; Zhang, H.; Cui, Q.; Sheng, N.; Yeung, L. W.; Guo, Y.; Sun, Y.; Dai, J., First report on the
- occurrence and bioaccumulation of hexafluoropropylene oxide trimer acid: An emerging concern.
- 530 Environmental science & technology **2017**, *51*, (17), 9553-9560.
- 531 23. Pan, Y.; Zhang, H.; Cui, Q.; Sheng, N.; Yeung, L. W.; Sun, Y.; Guo, Y.; Dai, J., Worldwide
- distribution of novel perfluoroether carboxylic and sulfonic acids in surface water. *Environmental science*
- 533 & technology **2018**, *52*, (14), 7621-7629.
- 534 24. Sun, M.; Arevalo, E.; Strynar, M.; Lindstrom, A.; Richardson, M.; Kearns, B.; Pickett, A.; Smith, C.;
- 535 Knappe, D. R., Legacy and emerging perfluoroalkyl substances are important drinking water
- 536 contaminants in the Cape Fear River Watershed of North Carolina. *Environmental science & technology*
- 537 *letters* **2016,** *3,* (12), 415-419.
- 538 25. Gebbink, W. A.; van Asseldonk, L.; van Leeuwen, S. P., Presence of emerging per-and
- polyfluoroalkyl substances (PFASs) in river and drinking water near a fluorochemical production plant in
- the Netherlands. Environmental science & technology 2017, 51, (19), 11057-11065.
- 541 26. Hill, J. T., Polymers from hexafluoropropylene oxide (HFPO). *Journal of Macromolecular*
- 542 Science—Chemistry **1974**, 8, (3), 499-520.
- 543 27. McCord, J.; Strynar, M., Identification of Per-and Polyfluoroalkyl Substances in the Cape Fear
- 544 River by High Resolution Mass Spectrometry and Nontargeted Screening. Environmental science &
- 545 *technology* **2019**, *53*, (9), 4717-4727.
- 546 28. McCord, J.; Newton, S.; Strynar, M., Validation of quantitative measurements and semi-
- quantitative estimates of emerging perfluoroethercarboxylic acids (PFECAs) and hexfluoroprolyene
- oxide acids (HFPOAs). Journal of Chromatography A 2018, 1551, 52-58.
- 549 29. Wang, Y.; Yu, N.; Zhu, X.; Guo, H.; Jiang, J.; Wang, X.; Shi, W.; Wu, J.; Yu, H.; Wei, S., Suspect and
- 550 nontarget screening of per-and polyfluoroalkyl substances in wastewater from a fluorochemical
- manufacturing park. Environmental science & technology 2018, 52, (19), 11007-11016.
- 30. Merino, N.; Qu, Y.; Deeb, R. A.; Hawley, E. L.; Hoffmann, M. R.; Mahendra, S., Degradation and
- removal methods for perfluoroalkyl and polyfluoroalkyl substances in water. *Environmental Engineering*
- *Science* **2016**, *33*, (9), 615-649.
- 555 31. Schaefer, C. E.; Andaya, C.; Burant, A.; Condee, C. W.; Urtiaga, A.; Strathmann, T. J.; Higgins, C.
- P., Electrochemical treatment of perfluorooctanoic acid and perfluorooctane sulfonate: Insights into
- 557 mechanisms and application to groundwater treatment. Chemical Engineering Journal 2017, 317, 424-
- 558 432.
- 559 32. Gole, V. L.; Fishgold, A.; Sierra-Alvarez, R.; Deymier, P.; Keswani, M., Treatment of
- 560 perfluorooctane sulfonic acid (PFOS) using a large-scale sonochemical reactor. Separation and
- 561 *Purification Technology* **2018,** *194*, 104-110.

- 562 33. Zhang, Z.; Chen, J.-J.; Lyu, X.-J.; Yin, H.; Sheng, G.-P., Complete mineralization of
- perfluorooctanoic acid (PFOA) by γ-irradiation in aqueous solution. *Scientific reports* **2014,** *4*, 7418.
- 564 34. Stratton, G. R.; Dai, F.; Bellona, C. L.; Holsen, T. M.; Dickenson, E. R.; Mededovic Thagard, S.,
- Plasma-based water treatment: efficient transformation of perfluoroalkyl substances in prepared
- solutions and contaminated groundwater. *Environmental science & technology* **2017**, *51*, (3), 1643-1648.
- 567 35. Trojanowicz, M.; Bojanowska-Czajka, A.; Bartosiewicz, I.; Kulisa, K., Advanced
- 568 Oxidation/Reduction Processes treatment for aqueous perfluorooctanoate (PFOA) and
- perfluorooctanesulfonate (PFOS)—A review of recent advances. Chemical Engineering Journal 2018, 336,
- 570 170-199.
- 571 36. Hori, H.; Nagano, Y.; Murayama, M.; Koike, K.; Kutsuna, S., Efficient decomposition of
- 572 perfluoroether carboxylic acids in water with a combination of persulfate oxidant and ultrasonic
- 573 irradiation. *Journal of Fluorine Chemistry* **2012,** *141,* 5-10.
- 574 37. Hori, H.; Yamamoto, A.; Koike, K.; Kutsuna, S.; Murayama, M.; Yoshimoto, A.; Arakawa, R.,
- 575 Photocatalytic decomposition of a perfluoroether carboxylic acid by tungstic heteropolyacids in water.
- 576 Applied Catalysis B: Environmental **2008**, 82, (1-2), 58-66.
- 577 38. Bao, Y.; Deng, S.; Jiang, X.; Qu, Y.; He, Y.; Liu, L.; Chai, Q.; Mumtaz, M.; Huang, J.; Cagnetta, G.,
- 578 Degradation of PFOA substitute: GenX (HFPO–DA ammonium salt): oxidation with UV/persulfate or
- reduction with UV/sulfite? *Environmental science & technology* **2018,** *52*, (20), 11728-11734.
- 580 39. Bao, Y.; Cagnetta, G.; Huang, J.; Yu, G., Degradation of hexafluoropropylene oxide oligomer acids
- as PFOA alternatives in simulated nanofiltration concentrate: Effect of molecular structure. Chemical
- 582 *Engineering Journal* **2020,** *382,* 122866.
- 583 40. Bentel, M. J.; Yu, Y.; Xu, L.; Li, Z.; Wong, B. M.; Men, Y.; Liu, J., Defluorination of per-and
- 584 polyfluoroalkyl substances (PFASs) with hydrated electrons: structural dependence and implications to
- 585 PFAS remediation and management. *Environmental science & technology* **2019,** *53*, (7), 3718-3728.
- 586 41. Liu, J.; Van Hoomissen, D. J.; Liu, T.; Maizel, A.; Huo, X.; Fernández, S. R.; Ren, C.; Xiao, X.; Fang,
- 587 Y.; Schaefer, C. E., Reductive defluorination of branched per-and polyfluoroalkyl substances with cobalt
- complex catalysts. *Environmental Science & Technology Letters* **2018,** *5*, (5), 289-294.
- 589 42. Seppelt, K., Trifluoromethanol, CF3OH. Angewandte Chemie International Edition in English
- 590 **1977,** *16*, (5), 322-323.
- 591 43. Christe, K. O.; Hegge, J.; Hoge, B.; Haiges, R., Convenient access to trifluoromethanol.
- 592 Angewandte Chemie International Edition **2007**, *46*, (32), 6155-6158.
- 593 44. Suenram, R.; Lovas, F.; Pickett, H., Fluoromethanol: Synthesis, microwave spectrum, and dipole
- 594 moment. *Journal of Molecular Spectroscopy* **1986,** *119*, (2), 446-455.
- 595 45. Maza, W. A.; Breslin, V. M.; Plymale, N. T.; DeSario, P. A.; Epshteyn, A.; Owrutsky, J. C.; Pate, B.
- 596 B., Nanosecond transient absorption studies of the pH-dependent hydrated electron quenching by HSO
- 597 3-. *Photochemical & Photobiological Sciences* **2019,** *18*, 1526-1532.
- 598 46. Sun, Z.; Zhang, C.; Xing, L.; Zhou, Q.; Dong, W.; Hoffmann, M. R., UV/nitrilotriacetic acid process
- as a novel strategy for efficient photoreductive degradation of perfluorooctanesulfonate. *Environmental*
- 600 science & technology **2018**, *52*, (5), 2953-2962.
- 601 47. Park, H.; Vecitis, C. D.; Cheng, J.; Dalleska, N. F.; Mader, B. T.; Hoffmann, M. R., Reductive
- degradation of perfluoroalkyl compounds with aquated electrons generated from iodide photolysis at
- 603 254 nm. *Photochemical & Photobiological Sciences* **2011,** *10,* (12), 1945-1953.
- 48. Tian, H.; Gao, J.; Li, H.; Boyd, S. A.; Gu, C., Complete defluorination of perfluorinated compounds
- by hydrated electrons generated from 3-indole-acetic-acid in organomodified montmorillonite. *Scientific*
- 606 reports **2016**, *6*, 32949.
- 607 49. Song, Z.; Tang, H.; Wang, N.; Zhu, L., Reductive defluorination of perfluorooctanoic acid by
- 608 hydrated electrons in a sulfite-mediated UV photochemical system. Journal of hazardous materials
- 609 **2013**, *262*, 332-338.